Al-Mustansiriyah Journal of Science
ISSN: 1814-635X (print), ISSN:2521-3520 (online) Volume 32, Issue 4, 2021 DOI: http://doi.org/10.23851/mjs.v32i4.1025

Research Article Open Access

Tribological Characteristics near Welding Limit for Petroleum Metal Pipelines

Atheer M. Jameel[1], Bahjat B. Kadhim[1*], Fadhil K. Farhan[2]

[1]Department of Physics, College of Science, Mustansiriyah University, Baghdad, IRAQ.
[2]Department of Medical Physics, College of Science, AL-Karkh University of Science, Baghdad, IRAQ.

*Correspondent contact: sci.phy.bbk@uomustansiriyah.edu.iq

Article Info

Received
15/06/2021

Accepted
01/08/2021

Published
20/11/2021

ABSTRACT

Welding process is one of the most widely applied processes in the industry. This is due to the ease of the process and it's a quantitative process. The addition of metallic powders to the welding area has not been widely emphasized as a solution to amelioration the tribology characteristic of the welding area therefore the effect of adding metallic powders (SnS nanoparticles) to the welding area on tribology properties was studied. This effect was studied at the values of coefficient of friction, coefficient of wear and wear rate by using the ring – on – disc sliding wear test equipment was used to study the tribological behavior of low carbon steel (A 106 grade B) as pure, 6010 welded and SnS- 6010 welded) under changing loads with constant velocity and in one hour for each run the dry condition at ambient temperature. The results show the coefficient of friction, coefficient of wear and wear rate increased with up load.

KEYWORDS: Wear; friction; metal pipelines; carbon steel; welding; pin-on-disc, disc-on-disc.

INTRODUCTION

The number of petroleum transport pipelines that are operated in changing and harsh conditions increases each year [1]. The environmental conditions as well as the difference aggressive of raw extractive materials and many derivatives petroleum productions are responsible for pipelines damages due to fatigue, mechanical damages, wear and corrosion [2-4]. The internal surfaces of transport welded pipelines petroleum and its derivatives can be deformed and damaged due to one of wear types as a consequence of the movement of many kinds of solid particles caused by petroleum and its derivatives flows. Apart from typical deformations in the form of weight loss as well as cracks, these phenomena can cause a reduction in the cross-section of the welding regions. These factors make it necessary to use protective coating layers on the internal surfaces of transport-welded pipelines, which improve the corrosion and wear resistance [5-7]. These coatings can be deposited by thermal spraying during the production of welded pipelines [8].

In particular, for natural gas, petroleum and its derivatives transportation pipelines over long distances, the use of pipes fabricated from high strength carbon steel (HSCS) such as (A 106 grade B) is very attractive from a technical and economical point of view. The basic advantages of (A 106 grade B) are high strength and toughness, higher strength/weight ratio, good formability and good weldability [2]. Weldability, being a very important technological factor of petroleum and its derivatives transportation pipelines carbon steels, depends on the metallurgical purity and total content of carbon and alloying elements. These factors govern the crack sensitivity of welded joints during the solidification process of a weld and wear tack place.

In some applications, like wear resistance the compounds coatings can be used [9,10]. However, chemical compounds commonly deposited layers are manufactured by the use of ceramics and metals. The ceramic coatings Al_2O_3/TiO_2, ZrO_2/CaO and SnS can be applied by a thermal spraying process [11-13]. The research works are focused on the improvement

of wear and corrosion resistance of welded layers of pipeline. One of the methods to reduce the wear of welded regions could be the use of coating technique which is made in an air environment.

In petroleum and its derivatives transportation pipelines applications, the specimens made up of welded pipelines have been subjected to mechanical rubbing action, which creates wear action. Wear is one kind of materials removal from the contacting surfaces due to relative motions between the two mating parts [14, 15]. The wear that occurred in the components was mainly based on the applied load, the operating temperature, and speed, the hardness of the material, the time duration of test, the atmospheric action, and the presence of foreign matters.

Tribological behavior, namely the wear rate, the wear coefficient, and the coefficient of friction, has clarified the wear rate of materials, which have played a major role in material removal [16 - 20]. This indicates the transfer of material from one surface to another owing to the relative motion between the contacting surfaces. A dry sliding wear test is the best experimental technique for many structural applications to find out the wear behavior.

According to the conditions of the Pin – on disc machine the wear rate (W_R) and wear coefficient (K) are calculated according to the following equation [21]:

$$W_R = \frac{\Delta W_V}{S_D} \quad (1)$$

$$K = \frac{W_V . H_V}{S_D . L} \quad (2)$$

Where: W_V, is the wear volume loss (mm^3) of the specimen before and after the wear test, H_V, Vickers hardness (N / mm^2), L, load (N) and S_D: is the sliding distance (m). The friction coefficient equation [22]:

$$\mu = \frac{Q}{r \times L} \quad (3)$$

Where: Q, is friction torque (m.N), L (load) applied on the sample (Newton) and r, is radius of counter face stainless steel disc in (m).

Wear is a foremost issue in the engineering field in which is one of the reasons of the failure during the usage of mechanical parts. Based on the literature, there was no report and detailed study on the dry sliding wear behavior of welded pipelines. Therefore, it is necessary to examine and study the wear behavior petroleum and its derivatives transportation pipelines. Therefore, the present research work was focused to optimize the essential wear parameters to determine the appropriate conditions and materials to be used for the petroleum and its derivatives transportation pipelines applications, which minimize the wear.

MATERIALS AND METHODOLOGY

The high strength carbon steel (HSCS) (A 106 grade B) was received from Ministry of Industry, Iraq. The chemical composition, the physical properties and the mechanical properties of as-received (HSCS) (A 106 grade B) are given in Table 1. Tin sulfide type (SnS) was synthesized using wet chemical method under standard conditions [23]. To get the (SnS) product, tin dichloride having the formula ($SnCl_2.2H_2O$) as the first source with sodium sulfide of the formula (Na_2S) as the second source are used to produce tin and sulfide respectively, with the present of deionized water, which is used as solvent. The weight of ($SnCl_2.2H_2O$) was (12) g and for (Na_2S) was (18) g according to appropriate molar ratio. The ($SnCl_2.2H_2O$) were dissolved in deionized water using magnetic stirrer for 2 hours at room temperature and (Na_2S) solution was dropping into the solution of $SnCl_2.2H_2O$). The precipitates (SnS) were wished with ethanol and dried at room temperature. According to this reaction (SnS) dark brown color nano powder were obtained.

Three models were prepared; the first as-received (A106 grade B) pipe was cut into several pieces of (ø40 × 10) mm as rings for doing the wear test. The second model is an ER6010 wire weld joint and the third model is the ER6010 wire weld joint with SnS nanoparticles added using the gas tungsten arc welding (GTAW) process after removing the cellulose cover of the wire. Each model was divided into three parts (R35x30x10) mm. Before the samples were cleaned with acetone and then the samples were polished as per the metallographic procedure. The samples were polished with different SiC grit papers (400, 600, 800, 1000, 1200, 2000 SiC grits/cm^2). Figure 1 show the specimen dimensions.

The ring – on – disc sliding wear test equipment was used to study the tribological behavior of high strength carbon steel (A 106 grade B) as pure, 6010 welded and SnS- 6010 welded) under the dry condition at ambient temperature. The work carried out by using a change loads from (70, 80, 90, 100, 110, 120 and 130) N for one hour with speed (120) rev/min and sliding distance (904.32) m.

The cylindrical counter disc was made of hardened stainless steel having 10 mm thickness and 40 mm diameter. The counter disc was initially ground and cleaned with acetone to eliminate the presence of oxide layers, foreign particles, and moisture. The prepared specimens for wear test were weighed before and after the test by which the mass loss was determined. Hardness and density testes were employed to determine the wear rate and wear coefficients based on the mass losses using (1) and (2) formula. The microstructural images in as-received condition and the worn surfaces were examined using the SEM (scanning electron microscope), with the AFM (atomic force microscopy) (done at Iran) to show how could be the surfaces after tribological testes.

Figure 1. Specimens dimensions.

RESULTS AND DISCUSSION

The X – ray diffraction is shown in Figure 2. The size of the nanoparticles was estimated using Scherer's formula based on the full width at half-maximum (FWHM) of the different diffraction peak with different values [24]:

$$A = \frac{0.94\lambda}{\beta cos\theta} \quad (4)$$

Where: A is crystallite size, β is the FWHM of the diffraction peak, λ is the wavelength of X-ray radiation and θ is the angle of diffraction. The average Scherrer size of these NPs is (70) nm. The inter-planar spacing measured were in good agreement with the spacing for the (110) (120), (111), (040), (041), (200), (141), (151), (122), (231), (042), (202), (023) and (133) planes for the orthorhombic SnS structure with JCPDS file NO. 00.039-0354.

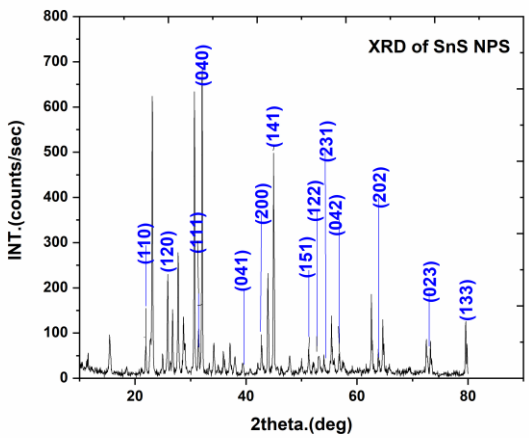

Figure 2. XRD pattern of SnS NPs.

Figure 3a shows the SnS nanopowder and Figure 3b shows the AFM surface image of SnS.

a

b

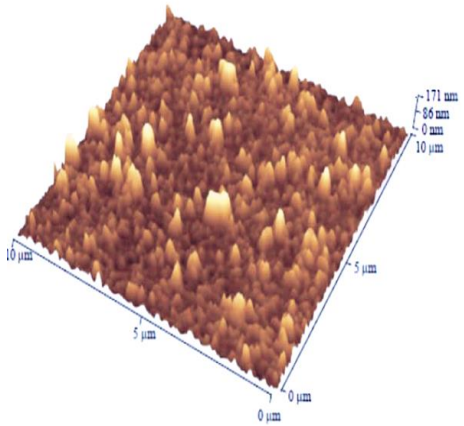

Figure 3. a- The SnS nanopowder, b- AFM 2D surface image of SnS.

A chemical analysis process [25] was conducted to find out the composition of the elements for the three models as in the Tables 1, 2 and 3

below. There are shown the elements included in the used steel and their proportions. The results in Table 3 show an increase in the percentage of sulfur and tin.

Table 1. Analytical chemical compositions of carbon steel A 106 GR B.

Elements	C	Mn	Si	P	S	Cr	Ni	Mo	V	Cu	Fe
Value%	0.23	0.76	0.33	0.017	0.019	0.32	0.19	0.08	0.04	0.24	Remaining

Table 2. Analytical chemical compositions of carbon steel ER 6010.

Element	C	Mn	Si	Cr	Ni	Mo	V	Fe
Value%	0.18	0.28	0.14	0.02	0.02	< 0.01	0.01	Remaining

Table 3. Analytical chemical compositions of carbon steel ER 6010 with SnS.

Element	C	Mn	Si	S	Cr	Ni	Mo	V	Sn	Fe
Value%	0.18	0.28	0.14	0.034	0.02	0.02	< 0.01	0.01	0.314	Remaining

Tables 4, 5 and 6 illustrate the results of the wear tests for the three models as below, (the coefficient of friction, coefficient of wear and wear rate). The values were increased for all specimens with increase in the amount of load leads to deform and fracture the surface films and allows for true contact and the large area contact, thus increasing the mass removed.

Table 4. Experimental results of sliding wear of A 106 Gr B.

Exp. No.	Mass difference (g)	Load (N)	Wear rate mm^3/m	Coefficient of wear (k)*(10^{-3})	Coefficient of friction (μ)
1	0.166	60	0.02379	0.4024	0.2333
2	0.209	70	0.02995	0.4351	0.3019
3	0.425	80	0.06092	0.7754	0.6150
4	0.563	90	0.08070	0.9140	0.8155
5	0.793	100	0.11367	1.1601	1.1500
6	0.868	110	0.12460	1.1548	1.2593
7	0.913	120	0.13090	1.1148	1.3256
8	1.017	130	0.14578	1.1464	1.4775

Table 5. Experimental results of sliding wear for welding wire ER 6010.

Exp. No.	Mass difference (g)	Load (N)	Wear rate mm^3/m	Coefficient of wear (k)*(10^{-3})	Coefficient of friction (μ)
1	0.139	60	0.0198	0.3361	0.1999
2	0.222	70	0.0317	0.4611	0.3200
3	0.373	80	0.0533	0.6790	0.5386
4	0.458	90	0.0655	0.7422	0.6621
5	0.640	100	0.0915	0.9341	0.9260
6	0.753	110	0.1077	1.0014	1.0905
7	0.874	120	0.1250	1.0649	1.2668
8	1.121	130	0.1604	1.2612	1.6253

Table 6. Experimental results of sliding wear for welding wire ER 6010 with SnS.

Exp. No.	Mass difference (g)	Load (N)	Wear rate mm^3/m	Coefficient of wear (k)*(10^{-3})	Coefficient of friction (μ)
1	0.123	60	0.0176	0.2967	0.1764
2	0.182	70	0.0260	0.3771	0.2617
3	0.269	80	0.0384	0.4791	0.3878
4	0.335	90	0.0479	0.5420	0.483
5	0.410	100	0.0530	0.5976	0.5925
6	0.507	110	0.0725	0.6718	0.732
7	0.602	120	0.8615	0.7318	0.870
8	0.694	130	0.0993	0.7793	1.004

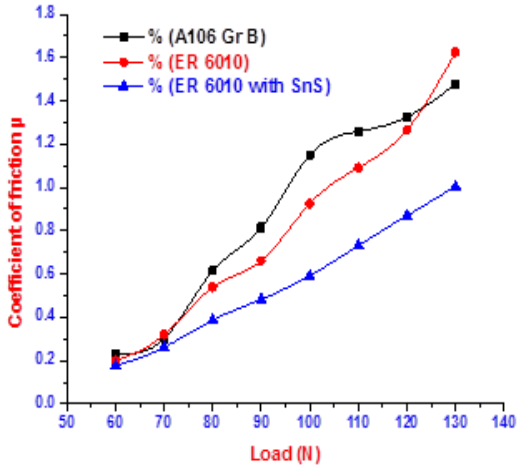

Figure 4. Coefficient of friction.

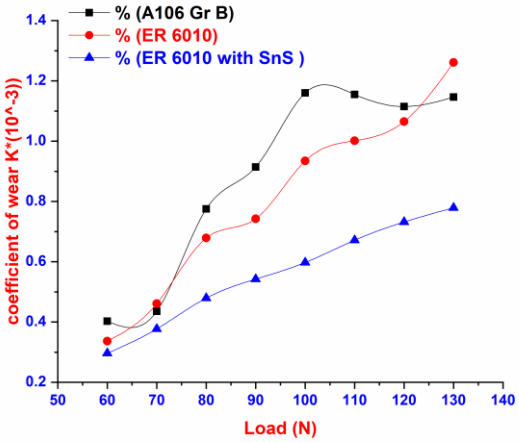

Figure 5. Coefficient of wear.

From the Figures 4 and 5, it can be shown the relationship between the coefficient of friction and the coefficient of wear with the load imposed on the sample for the dependent models which is shown a decrease in the friction coefficient and the coefficient of wear of the (ER6010) alloy with the addition of SnS nanoparticles compared with the original metal and the ER6010 alloy which has the highest friction coefficient, and that because SnS plays as lubricant element.

Moreover, the resin for this result the SnS was increasing the durability and efficiency because wear and friction coefficient obtained decreasing in sample (ER6010WITH SnS).

Figure 6 illustrates the sample ER6010+SnS NPS show improvement in the wear rate compared with the pure metal and the ER 6010 alloy, this is due to the increase in the load because the wear rate proportional to the distance slid, which leads to an increase in the amount of erosion the wear rate for three curves is fairly constant.

Figure 7 represents the digital microscopy picture, sever wear occurs in load (7) Kg for pure metal and the ER6010 alloy and the module (ER6010 + SnS). It showed the formation of the oxide film as a result of mild wear, which leads to a decrease in the volume of the material removed and thus to a decrease in the wear and friction coefficient as well as in the wear rate.

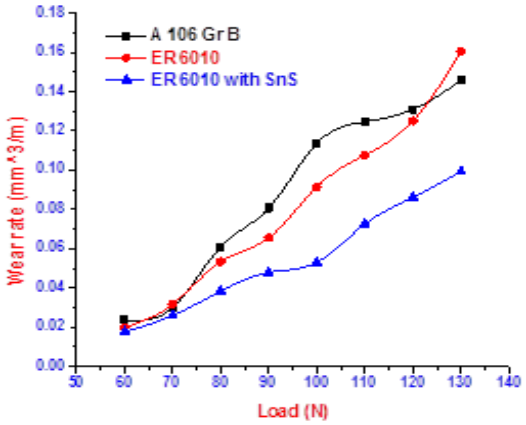

Figure 6. Wear rate A106 Gr B, ER 6010 and ER 6010 with SnS.

Digital microscopy for pure metal under load 7 kg

Digital microscopy for ER 6010 alloy under load 7 kg

Digital microscopy for ER 6010 alloy + SnS under load 7 kg

Figure 7. Microscopy picture, sever wear occurs in load (7) Kg for pure metal, ER6010 alloy and (ER6010 + SnS).

In Figure 8, the digital microscopy images shown more sever wear occurs in load (10) Kg for the pure metal and the ER6010 alloy which it leads to more plowing depth, but the module ER6010 +SnS. It showed the less ploughing with superficial scratches as a result of the action of SnS which it leads to a decrease in the volume of the material removed and thus to a decrease in the wear and friction coefficient as well as in the wear rate.

Digital microscopy for A 106 Gr B under load 10 kg. | Digital microscopy for ER6010 alloy under load 10 kg. | Digital microscopy for ER6010 alloy + SnS under load 10 kg.

Figure 8. Microscopy images shown more sever wear occur in load (10) Kg for the pure metal and the ER6010 alloy.

The digital microscopy picture for more sever wear occurs in load (13) Kg for the pure metal and the ER6010 alloy are shown in Figure 9, which it leads to plastically deformation and more ploughing depth, but the module ER6010 + SnS It showed the less ploughing with superficial scratches plastically deformation as a result to sever wear.

Figure 10 represents SEM images for pure metal and the ER6010 alloy, but the module ER6010 +SnS under load (130), which appears the samples nanostructures after wear tests.

Digital microscopy for pure metal under load 13 kg. | Digital microscopy for ER6010 alloy under load 13 kg. | Digital microscopy for ER6010 alloy + SnS under load 13 kg.

Figure 9. Digital microscopy picture for more sever wear occurs in load (13) Kg for the pure metal and the ER6010 alloy.

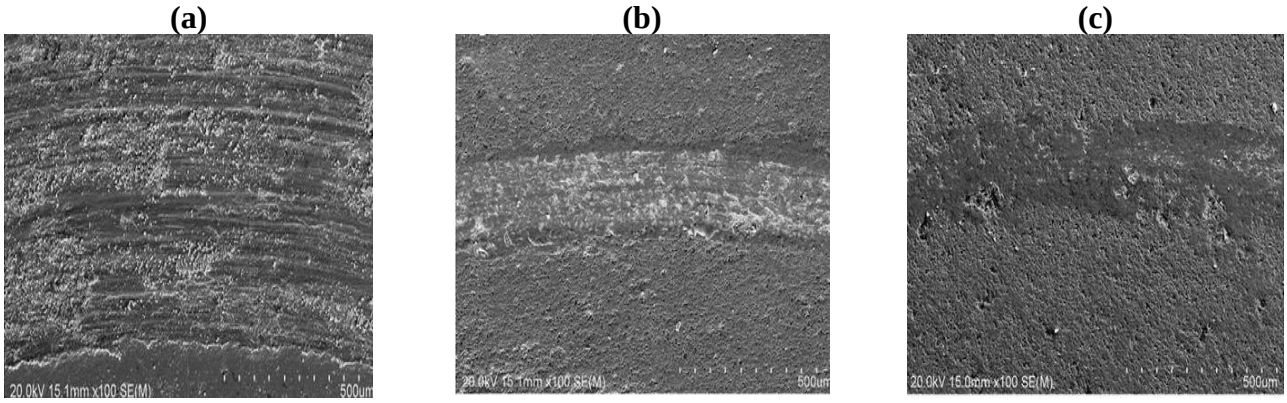

Figure 10. SEM images for: (a) pure metal, (b) ER6010 welding alloy and (c) ER6010 welding alloy + SnS.

CONCLUSIONS

The presence of normal load indeed affects the friction force, and wear rate considerably. The values of friction coefficient, coefficient of wear and the wear rates increase with the increase of normal load (but not always). Wear tests of three samples demonstrated that the SnS nanoparticles reduced the wear and friction coefficients as well as the wear rate despite the increased loads as they reduced the size of the material removed and also by reducing surface ploughing.

REFERENCES

[1] Węglowski, M. St, S. Dymek, M. Kopyściański, J. Niagaj, J. Rykała, Wim De Waele, and Stijn Hertelé. "A comprehensive study on the microstructure and mechanical properties of arc girth welded joints of spiral welded high strength API X70 steel pipe." *Archives of Civil and Mechanical Engineering* 20, no. 1 (2020): 1-18.

[2] Hernandez-Rodriguez, M. A. L., D. Martinez-Delgado, R. Gonzalez, A. Pérez Unzueta, R. D. Mercado-Solís, and J. Rodriguez. "Corrosive wear failure analysis in a

natural gas pipeline." *Wear* 263, no. 1-6 (2007): 567-571.

[3] Dehghani, Ayoub, and Farhad Aslani. "A review on defects in steel offshore structures and developed strengthening techniques." In *Structures*, vol. 20, pp. 635-657. Elsevier, 2019.

[4] Price, Seth J., and Rita B. Figueira. "Corrosion protection systems and fatigue corrosion in offshore wind structures: current status and future perspectives." *Coatings* 7, no. 2 (2017): 25.

[5] Papatheocharis, Theocharis, Gregory C. Sarvanis, Philip C. Perdikaris, and Spyros A. Karamanos. "Fatigue of welded tubular X-joints in offshore wind platforms." In *International Conference on Offshore Mechanics and Arctic Engineering*, vol. 58790, p. V004T03A024. American Society of Mechanical Engineers, 2019.

[6] Kong, Xiangfeng, Jing Lv, Nan Gao, Xin Peng, and Jing Zhang. "An experimental study of galvanic corrosion on an underwater weld joint." *Journal of Coastal Research* 84 (2018): 63-68.

[7] Liang, Liang, Youxia Pang, Zongming Zhu, Yong Tang, and Yanghui Xiang. "Influencing factors of various combinations of abrasion, cavitation, and corrosion caused by multiphase flow impact." *Transactions of the Canadian Society for Mechanical Engineering* 44, no. 2 (2019): 234-243.

[8] López-Ortega, A., J. L. Arana, E. Rodríguez, and R. Bayón. "Corrosion, wear and tribocorrosion performance of a thermally sprayed aluminum coating modified by plasma electrolytic oxidation technique for offshore submerged components protection." *Corrosion Science* 143 (2018): 258-280.

[9] Vereschaka, A. A., M. A. Volosova, A. D. Batako, A. S. Vereshchaka, and B. Ya Mokritskii. "Development of wear-resistant coatings compounds for high-speed steel tool using a combined cathodic vacuum arc deposition." *The International Journal of Advanced Manufacturing Technology* 84, no. 5-8 (2016): 1471-1482.

[10] Yu, Jinku, Yuehua Wang, XiCan Zhao, Qinyang Li, Qi Qiao, Jia Zhao, and Sen Zhai. "Wear resistance of ni-based alloy coatings." *Advances in Materials Science and Engineering* 2019 (2019).

[11] Espallargas, N. "Introduction to thermal spray coatings." In *Future Development of Thermal Spray Coatings*, pp. 1-13. Woodhead Publishing, 2015.

[12] Berger, Lutz-Michael. "Application of hardmetals as thermal spray coatings", *International Journal of Refractory Metals and Hard Materials* 49 (2015): 350-364.

[13] Rahim, M. S. A., S. Nor Hayati, and H. Luay Bakir. "Plasma spray ceramic coating and measurement of developed coating behaviour." *International Journal of Precision Technology* 1, no. 2 (2009): 163-172.

[14] Swain, Biswajit, Subrat Bhuyan, Rameswar Behera, Soumya Sanjeeb Mohapatra, and Ajit Behera. "Wear: A Serious Problem in Industry." In *Tribology*. IntechOpen, 2020.

[15] Igartua, Amaya, Raquel Bayon, Ana Aranzabe, and Javier Laucirica. "Tribology: The Tool to Design Materials for Energy-Efficient and Durable Products and Process." In *Friction, Lubrication and Wear*. IntechOpen, 2019.

[16] Georgescu, Constantin, Lorena Deleanu, and George Catalin Cristea. "Tribological behavior of soybean oil." In *Soybean-Biomass, Yield and Productivity*. IntechOpen, 2018.

[17] Ma, Yunhai, Yucheng Liu, and Jin Tong. "Bamboo Wear and Its Application in Friction Material." In *Bamboo-current and future prospects*. IntechOpen, 2017.

[18] Kawada, Shouhei, Seiya Watanabe, Shinya Sasaki, and Masaaki Miyatake. "Tribochemical reactions of halogen–free ionic liquids on nascent steel surface." *Recent advances in ionic liquids. IntechOpen* (2018): 47-65.

[19] Berradja, Abdenacer. "A Tribo-Electrochemical Investigation of Degradation Processes in Metallic Glasses." *Metallic Glasses: Properties and Processing* (2018): 111.

[20] Di Puccio, Francesca, and Lorenza Mattei. "Biotribology of artificial hip joints." *World journal of orthopedics* 6, no. 1 (2015): 77.

[21] Salim, Faiza M. "Tribological and Mechanical Characteristics of Dental Fillings Nanocomposites." *Energy Procedia* 157 (2019): 512-521.

[22] Olaru, Dumitru, George C. Puiu, Liviu C. Balan, and Vasile Puiu. "A new model to estimate friction torque in a ball screw system." In *Product engineering*, pp. 333-346. Springer, Dordrecht, 2004.

[23] Suresh, S. "wet chemical synthesis of Tin sulfide nanoparticles and its characterization." *International Journal of Physical Sciences* 9, no. 17 (2014): 380-385.

[24] Mousa, Fatin H., Ali S. Mahdi, Bahjat B. Kadhim, and Ali M. Ali. "Technological characteristics of perovskite solar cell windows using CdS–wurtzoid structure." In *AIP Conference Proceedings*, vol. 2190, no. 1, p. 020032. AIP Publishing LLC, 2019.

[25] Cantarelli, Miguel Angel, Roberto Gerardo Pellerano, Eduardo Jorge Marchevsky, and José Manuel Camiña. "Quality of honey from Argentina: study of chemical composition and trace elements." (2008).